J Arid Land (2023) 15(7): 842–857
https://doi.org/10.1007/s40333-023-0060-1

Science Press Springer-Verlag

Stem sap flow of *Haloxylon ammodendron* at different ages and its response to physical factors in the Minqin oasis-desert transition zone, China

QIANG Yuquan[1,2,3], ZHANG Jinchun[1,2,3*], XU Xianying[1,2,3], LIU Hujun[1,2], DUAN Xiaofeng[1,2]

[1] Minqin National Station for Desert Steppe Ecosystem Studies, Minqin 733300, China;
[2] Gansu Desert Control Research Institute, Lanzhou 730000, China;
[3] College of Forestry, Gansu Agricultural University, Lanzhou 730000, China

Abstract: *Haloxylon ammodendron*, with its tolerance of drought, high temperature, and salt alkali conditions, is one of the main sand-fixing plant species in the oasis-desert transition zone in China. This study used the TDP30 (where TDP is the thermal dissipation probe) to measure hourly and daily variations in the stem sap flow velocity of *H. ammodendron* at three age-classes (10, 15, and 20 years old, which were denoted as *H*10, *H*15, and *H*20, respectively) in the Minqin oasis-desert transition zone, China, from May through October 2020. By simultaneously monitoring temperature, relative humidity, photosynthetically active radiation, wind speed, net radiation, rainfall, and soil moisture in this region, we comprehensively investigated the stem sap flow velocity of different-aged *H. ammodendron* plants (*H*10, *H*15, and *H*20) and revealed its response to physical factors. The results showed that, on sunny days, the hourly variation curves of the stem sap flow velocity of *H. ammodendron* plants at the three age-classes were mainly unimodal. In addition, the stem sap flow velocity of *H. ammodendron* plants decreased significantly from September to October, which also delayed its peak time of hourly variation. On rainy days, the stem sap flow velocity of *H. ammodendron* plants was multimodal and significantly lower than that on sunny days. Average daily water consumption of *H. ammodendron* plants at *H*10, *H*15, and *H*20 was 1.98, 2.82, and 1.91 kg/d, respectively. Temperature was the key factor affecting the stem sap flow velocity of *H. ammodendron* at all age-classes. Net radiation was the critical factor influencing the stem sap flow velocity of *H. ammodendron* at *H*10 and *H*15; however, for that at *H*20, it was vapor pressure deficit. The stem sap flow velocity of *H. ammodendron* was highly significantly correlated with soil moisture at the soil depths of 50 and 100 cm, and the correlation was strengthened with increasing stand age. Altogether, our results revealed the dynamic changes of the stem sap flow velocity in different-aged *H. ammodendron* forest stands and its response mechanism to local physical factors, which provided a theoretical basis for the construction of new protective forests as well as the restoration and protection of existing ones in this region and other similar arid regions in the world.

Keywords: *Haloxylon ammodendron*; stem sap flow; stand age; soil moisture; water consumption; Minqin oasis-desert transition zone

Citation: QIANG Yuquan, ZHANG Jinchun, XU Xianying, LIU Hujun, DUAN Xiaofeng. 2023. Stem sap flow of *Haloxylon ammodendron* at different ages and its response to physical factors in the Minqin oasis-desert transition zone, China. Journal of Arid Land, 15(7): 842–857. https://doi.org/10.1007/s40333-023-0060-1

*Corresponding author: ZHANG Jinchun (E-mail: junchunzhang@163.com)
Received 2022-12-01; revised 2023-03-18; accepted 2023-03-21

1 Introduction

The oasis-desert transition zone is the most intensive and prominent area of oasis and desert inter-conversion activities (Pan, 2000; Cao et al., 2021). This type of area is therefore extremely fragile and sensitive, being vulnerable to human activities and quite difficult to restore once degraded or destroyed (Ding, 2018; Lu et al., 2023). Moreover, this zone was also the interface area with the most frequent material cycle, energy flow, and information exchange between oasis and desert ecosystems (Thomas et al., 2006; Chang et al., 2007).

Haloxylon ammodendron is a deciduous shrub and small tree in the family Amaranthaceae, being a C_4 plant species native to Central Asian desert habitats (Li et al., 2015; He et al., 2018). Further, it is a key functional species for establishing windbreaks and sand-fixation forests in the Minqin oasis-desert transition zone, China (Zhu and Jia, 2011; Zhang et al., 2019). Due to the impact of various factors, such as climate change and human activities, both the groundwater level and soil moisture in this transition zone are declining (Wang et al., 2015; Wang et al., 2023). Nearly 60% of the existing 44,600 hm^2 of the *H. ammodendron* shelterbelt has suffered from poor growth or degradation, which greatly impairs its windbreak and sand fixation functioning. This ongoing degradation of *H. ammodendron* vegetation threatens the survival and development of the Minqin oasis (Yang et al., 2020).

The water consumed via plant transpiration is a fundamental component of the water cycle and energy balance of forest ecosystems, being a crucial indicator reflecting the water status of plants as well as a key contributing factor affecting regional and even global climate dynamics (Ning et al., 2020). Recently, Poyatos et al. (2021) summarized the existing body of research findings on the relationship between stem sap flow and transpiration; they believed that under normal circumstances, the stem sap flow could accurately reflect the transpiration efficiency and water use status of a single plant in each time period. Accordingly, studying the responses in the stem sap flow of different-aged *H. ammodendron* plants to physical factors is of great significance to better understand how the water consumption of *H. ammodendron* changes through ontogeny. In China, research on *H. ammodendron* in the Minqin oasis-desert transition zone has focused on leaf photosynthesis, transpiration, and water use efficiency (Hu et al., 2021), drought tolerance (Lü et al., 2019), and root morphological characteristics (Jiang et al., 2018). However, a systematic investigation of water consumption per plant and its relationship with external meteorological factors and soil moisture during the whole growing season of *H. ammodendron* at different ages in the Minqin oasis-desert transition zone has yet to be reported. By analyzing the dynamic changes in the stem sap flow of different-aged *H. ammodendron*, not only can we grasp the water consumption law of *H. ammodendron* during its growth process but also can we reveal its response mechanism under self-thinning when adapting to local changes in arid environments; the knowledge gains can be useful for effectively carrying out protection and restoration work for different-aged *H. ammodendron* plants.

To that end, taking a typical sand-fixing plant in the Minqin oasis-desert transition zone in China as the object of research, this study continually measured the stem sap flow of *H. ammodendron* at different ages across the entire growing season. External physical factors were simultaneously measured to analyze the changes in the stem sap flow of different-aged *H. ammodendron* and the correlation between stem sap flow and physical factors, to better understand the age-dependent characteristics of water consumption by this species and how this responds to those abiotic factors. This study's findings are expected to provide a theoretical basis for the restoration and protection of degraded *H. ammodendron* plants and the establishment of new *H. ammodendron* shelterbelt.

2 Materials and methods

2.1 Study area

The study area (Minqin oasis-desert transition zone; 39°08′56″–39°09′02″N,

103°36′54″–103°38′01″E; Fig. 1) is located near the Minqin Desert Control Research Station at the southeastern edge of the Badain Jaran Desert, China, at an elevation of 1380 m. This region has a typical continental climate, with an annual average temperature of 7.3°C and an effective cumulative temperature greater than 10.0°C of 3289.1°C. Average annual precipitation is 110.0 mm, mainly falling from July to September, with at least 2640.0 mm of potential evaporation. The frost-free period lasts 168 d and there are 3181 h of sunshine per year, with 630 kJ/cm^2 of solar radiation; the year-round prevailing northwest wind has an annual average speed of 4.1 m/s. Soil here is mostly sandy, with poor nutrients and serious wind erosion. The landform is mostly semi-fixed sandy land interspersed with sand dunes at 3–10 m in height. From 2019 to 2022, the buried depth of groundwater in the study area was between 22.95 and 23.41 m. Vegetation of the study area is dominated by xerophyte shrubs, semi-shrubs, and annual and perennial herbs, namely consisting of the shrubs *H. ammodendron*, *Nitraria tangutorum*, and *Artemisia arenaria*, and the herbs *Phragmites australis*, *Kali collinum*, *Halogeton glomeratus*, and *Agriophyllum squarrosum*.

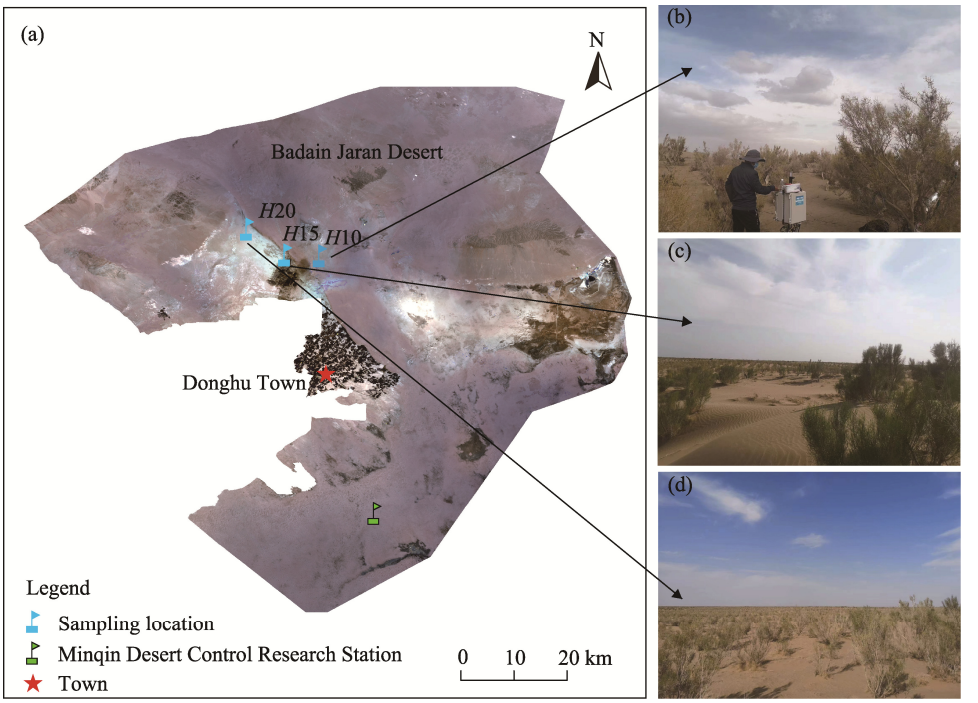

Fig. 1 Overview of the Minqin oasis-desert transition zone at the southeastern edge of the Badain Jaran Desert and locations of sampled *H. ammodendron* forest stands as well as the field photos of *H*10 (b), *H*15 (c) and *H*20 (d). *H*10, *H*15, and *H*20 are *H. ammodendron* forest stands with different afforestation ages of 10, 15, and 20 years old, respectively. The Landsat 8 OLI-TIRS images were downloaded from Geospatial Data Cloud.

2.2 Experimental design

According to the elapsed time since they were planted, we selected three artificial *H. ammodendron* forest stands with different afforestation ages of 10, 15, and 20 years old (hereon named *H*10, *H*15, and *H*20, respectively) in the Minqin oasis-desert transition zone for study. Four representative *H. ammodendron* individuals (samples) that were growing well and looked healthy were chosen at each age class (see Table 1 for their specific parameters). The plant height of *H. ammodendron* was measured with a tower ruler, the crown width and distance between plants and rows were determined with a tape measure, and the stem ground diameter was measured with a vernier caliper. Using the TDP30 (where TDP is the thermal dissipation probe) (Rainroot Scientific Limited, Beijing, China), we measured the stem sap flow velocity for each individual from 1 May to 30 October, 2020. The TDP30 was applied to a smooth spot at 40 cm

aboveground on the stem's east side. Specifically, this measuring spot was first sanded with sandpaper, and then the probe was drilled and inserted into the polished spot with a drill needle matching the probe. Once installed, the probe was wrapped with a special plastic fixing sponge, and the latter was wrapped in silver radiation-proof aluminum platinum paper; thermal insulation cotton was placed on the ground around the probe to reduce the influence of ground temperature on its measurements. A CR1000 data collector (CR1000, Campbell Scientific Inc., Logan, UT, USA) was connected to the probe to collect data every 1 min every day throughout the observation period.

Table 1 Basic information of the sampled *Haloxylon ammodendron* at different ages (*H*10, *H*15, and *H*20)

Forest stand	No. of the individual	Probe model	Plant height (cm)	Stem ground diameter (cm)	Canopy diameter (N×S) (cm×cm)	Stand density (plants/hm^2)	Soil moisture at 0–100 cm depth (%)
*H*10	S1	TDP30	130	3.27	135×105	853.00±172.57	2.00±1.19
	S2	TDP30	170	3.41	165×150		
	S3	TDP30	165	3.72	160×140		
	S4	TDP30	170	3.81	150×155		
*H*15	S1	TDP30	250	5.08	260×190	88.00±162.86	2.90±1.45
	S2	TDP30	290	5.33	230×280		
	S3	TDP30	290	5.85	300×290		
	S4	TDP30	380	7.85	385×370		
*H*20	S1	TDP30	222	8.49	205×140	46.00±247.09	2.03±1.42
	S2	TDP30	310	8.86	155×180		
	S3	TDP30	280	9.13	210×195		
	S4	TDP30	251	9.54	251×147		

Note: *H*10, *H*15, and *H*20 are *H. ammodendron* forest stands with different afforestation ages of 10, 15, and 20 years old, respectively. S1 to S4 are the numeric labels of sampled plants in each sampled forest stand. N, north; S, south. Mean±SE.

2.3 Determination of the stem sap flow and water consumption of *H. ammodendron*

Stem sap flux density (i.e., stem sap flow velocity) was calculated on the basis of the empirical formula in Granier (1987):

$$F_d = \alpha k^{\beta} = 119.99\times10^{-6}\left\{\left(\Delta T_{\max} - \Delta T\right)/\Delta T\right\}^{1.231}, \quad (1)$$

where F_d is the stem sap flux density (cm^3/(cm^2·h)); k is a dimensionless unit; α and β are the coefficients, depending on the thermal coefficient; $\Delta T_{\max}$ denotes the maximum temperature difference between the two probes when there was no stem sap flow (°C); and ΔT is the temperature difference between the two probes when there existed stem sap flow (°C). The measurement time without stem sap flow was set to 00:00–01:00 (LST) in May, July, August, September, and October, and to 03:00–04:00 in June.

The daily transpiration of a single individual (sample) was calculated as follows:

$$Q = F_d \times A_s \times T, \quad (2)$$

$$A_s = 0.699\mathrm{e}^{0.349x}\left(R^2 = 0.966\right), \quad (3)$$

where Q is the daily transpiration (cm^3); A_s is the sapwood area (cm^2); T refers to 24 h of time in a given day; and x is the *H. ammodendron* diameter (cm). The sapwood area was calculated using the exponential function described in Zhang et al. (2017).

Finally, a mass formula ($m=\rho\times V/1000$, where m is the water consumption (kg), ρ is the density of water (g/cm^3), taking 1 g/cm^3 in this study, and V is the daily transpiration (cm^3), equivalent to Q) was used to calculate water consumption, by which the daily transpiration (Q; cm^3) was converted to water consumption.

2.4 Determination of meteorological factors

Three portable weather stations were deployed synchronously at the sampled forest stands to monitor local meteorological factors. These stations recorded daily average temperature (°C), relative humidity (RH; %), photosynthetically active radiation (PAR; μmol/(s·m^2)), surface net radiation (*Rn*; W/m^2), daily average wind speed at 2 m above the ground (m/s), and rainfall (mm) every 10 min, from May through October 2020. The calculation method of vapor pressure deficit (VPD) was referred to Zheng and Wang (2015) and Zhang et al. (2016).

2.5 Determination of soil moisture

A series of EC-5 soil moisture sensors (Ecotek Technology Limited, Beijing, China) were installed at the depths of 5, 20, 50, 100, and 150 cm belowground at each *H. ammodendron* forest stand and connected to EM50 data collectors (Ecotek Technology Limited, Beijing, China). Data were downloaded from EM50 data collectors by using ECH_2O Utility software (Ecotek Technology Limited, Beijing, China). After the installation was completed, near to where each sensor was positioned, soil bulk density was taken and the actual soil moisture was measured to calibrate the moisture probe error. The measurement period spanned from April to November 2020, with the data measurement interval of 1 h.

2.6 Data processing and calculations

Under sunny conditions, based on the stem sap flow velocity data of *H. ammodendron* at each age-classes (*H*10, *H*15, and *H*20), we selected a day with more stable changes from consecutive days that showed similar trends for each month, to represent the stem sap flow variations of *H. ammodendron* in that month. Under rainy conditions, a day with high rainfall and significant changes in the stem sap flow velocity of *H. ammodendron* for each stand age was selected for analysis. Next, the average value of four *H. ammodendron* individuals at each age class was used to express the age-specific trend in changed stem sap flow velocity (Table 1). The hourly and daily variation data of the stem sap flow velocity of *H. ammodendron* were obtained by adding up the monitoring data every 10 min. SPSS 16.0 software (SPSS Inc., Chicago, IL, USA) and Microsoft Excel 2019 software were used for the statistical analysis.

2.7 Response of the stem sap flow of *H. ammodendron* to physical factors

A structural equation model (SEM) was used to determine the relative response of the stem sap flow of different-aged *H. ammodendron* individuals to meteorological factors and the size of the weights accounted for. The model-building process was divided into five steps: constructing a theoretical model, formulating research hypotheses, testing the reliability and validity, assessing the model fitness, and adjusting and revising the model as needed. Daily values of the stem sap flow velocity of *H. ammodendron* individuals at *H*10, *H*15, and *H*20 were used as the criterion layer, and temperature, RH, *Rn*, wind speed, and VPD were used as the indicator layer, assuming that all these physical factors could exert a driving effect on the stem sap flow. MPLUS 8.0 software (Muthen & Muthen, Los Angeles, CA, USA) was used to test the discriminant validity of the SEM. The data were assessed for reliability by applying Kronbach and Kaiser-Meyer-Olkin (KMO) tests, to determine whether the data could be used for structural equation modeling. The model fit was evaluated by the chi-square free ratio (χ^2/df), comparative fit index (CFI), Tucker-Lewis index (TLI), root mean square error of approximation (RMSEA), and standardized root mean square residual (SRMR) metrics. Based on the path coefficients in the path diagram of the SEM, we used the Analytic Hierarchy Process (AHP) to obtain the weighted results of each meteorological factor. Correlation analysis between soil moisture and stem sap flow velocity was done using SPSS 16.0 software.

3 Results

3.1 Dynamics of meteorological factors

The changes in each meteorological factor (temperature, RH, PAR, wind speed, VPD, rainfall,

and *Rn*) during the growing season (1 May–31 October, 2020) were presented statistically (Fig. 2). For temperature, its maximum value (30.8°C) occurred in early July and its minimum value (–4.5°C) in October. For RH, it fluctuated between 10% and 97% from May to July, and between 26% and 91% from August to October. For PAR, its overall trend was one of increasing at first and then decreasing, peaking at 940 μmol/(s·m^2) in June. For wind speed, its highest daily average reached 3.7 m/s (in May), and its lowest value was 0.3 m/s (in May). The wind frequency increased from August to September, and generally the daily average wind speed fluctuated greatly. For VPD, its overall trend was of increasing then decreasing, peaking at 2.6 kPa in June. The total rainfall was 55.5 mm during the whole growing season in 2020 and the highest daily rainfall of 7.1 mm occurred on 30 September. *Rn* fluctuated with multiple peaks evident; i.e., 172.9 W/m^2 in June, 179.2 W/m^2 in July, and 175.0 W/m^2 in September.

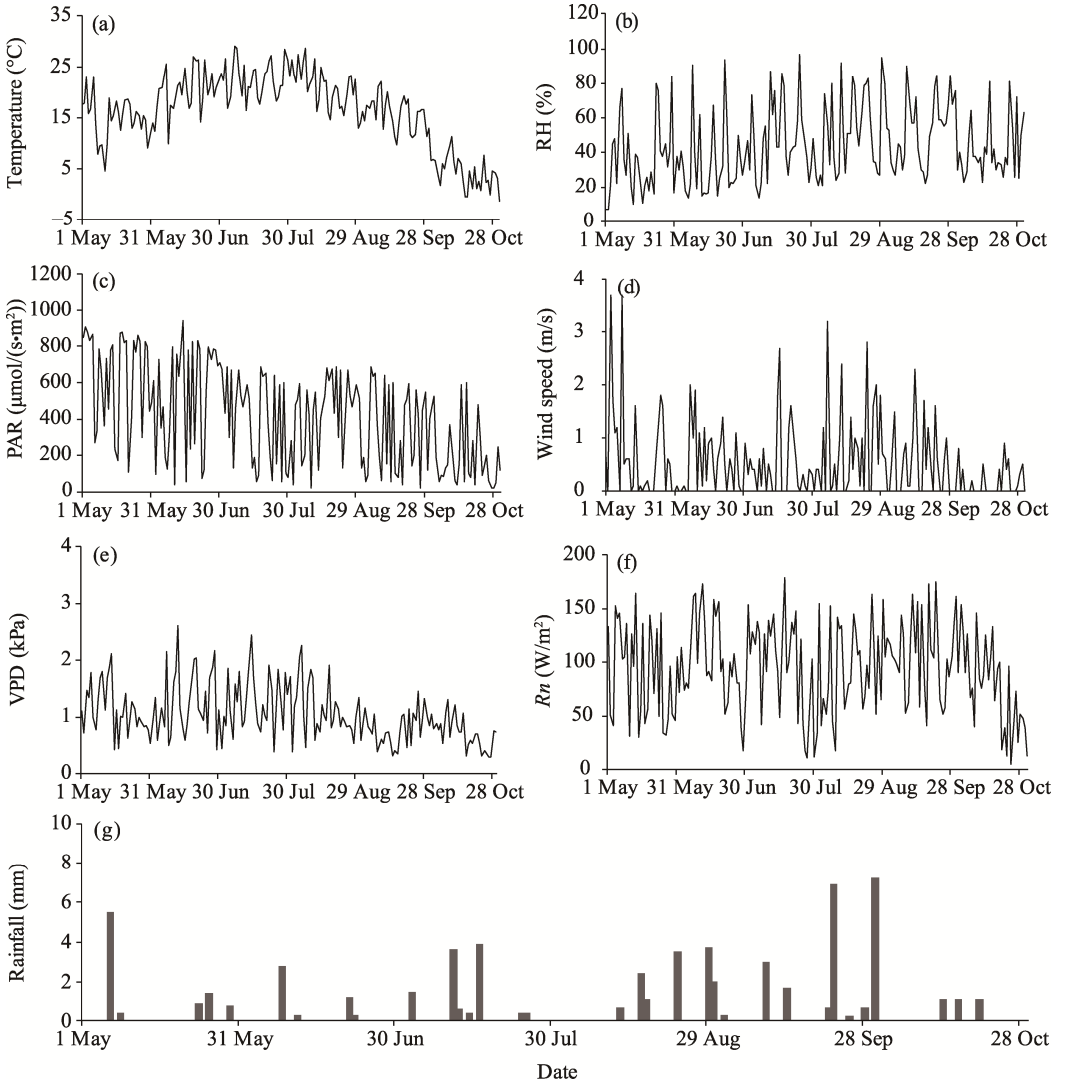

Fig. 2 Dynamics of seven meteorological factors during the growing season (from 1 May to 31 October) of 2020. (a), temperature; (b), relative humidity (RH); (c), photosynthetically active radiation (PAR); (d) wind speed; (e), vapor pressure deficit (VPD); (f), surface net radiation (*Rn*); (g), rainfall.

3.2 Dynamics of the stem sap flow velocity in *H. ammodendron* at different ages

3.2.1 Hourly dynamics of the stem sap flow velocity of different-aged *H. ammodendron* on sunny days

Hourly dynamics in the stem sap flow velocity of *H. ammodendron* on six typical sunny days

from May to October (20 May, 17 June, 15 July, 20 August, 16 September, and 21 October) were analyzed to reveal hourly variation characteristics of the stem sap flow velocity of *H. ammodendron* at different ages (*H*10, *H*15, and *H*20) (Fig. 3). In June, the peak value of the stem sap flow velocity of *H. ammodendron* at *H*10 and *H*15 arose between 08:50 and 09:00, whereas that at *H*20 was delayed to 14:10. In July, the start-up time of the stem sap flow of *H. ammodendron* at *H*10 and *H*15 was 05:40–06:00, and the peak value appeared at 08:50–09:20. The start-up time of the stem sap flow for the plants at *H*20 in July was 08:00, for which the peak occurred at 11:20. In August, the start-up time of the stem sap flow of *H. ammodendron* at all three age-classes happened between 07:00 and 07:30, whose peak appeared between 11:40 and 12:00 for *H*15 and *H*20 but later at 13:30 for *H*10. In September, the start-up time of the stem sap flow of *H. ammodendron* at *H*10 and *H*15 was 02:30, whose peaks both appeared between 13:20 and 13:30, whereas that was much later (at 07:30) for *H*20 though it peaked sooner at 11:10. The start-up time of the stem sap flow of *H. ammodendron* in October was 02:10–02:30 for *H*10 and *H*15, and 07:40 for *H*20; for *H. ammodendron* plants at the three age-classes (*H*10, *H*15, and *H*20), the corresponding peak values differed considerably, appearing at 15:50, 10:40, and 12:30, respectively.

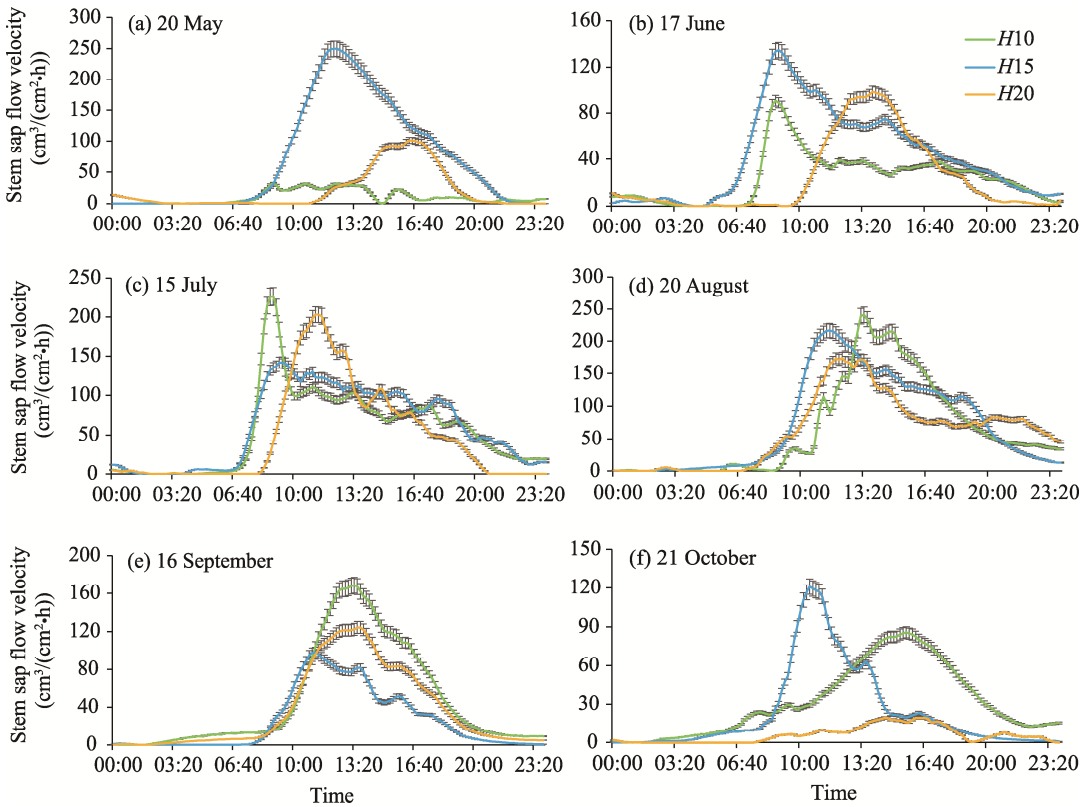

Fig. 3 Hourly dynamics in the stem sap flow velocity of *H. ammodendron* at different ages (*H*10, *H*15, and *H*20) on sunny days of 20 May (a), 17 June (b), 15 July (c), 20 August (d), 16 September (e), and 21 October (f). Bars mean standard errors.

3.2.2 Hourly dynamics of the stem sap flow velocity of different-aged *H. ammodendron* on rainy days

In each month from May through August, four typical rainy days with high rainfall amounts (i.e., 26 May, 20 June, 10 July, and 24 August) were selected to analyze the effect of rainfall on the stem sap flow velocity of *H. ammodendron*, by examining its hourly variation (Fig. 4). Evidently, the stem sap flow velocity of *H. ammodendron* on rainy days was significantly lower than that on sunny days, and there was a significant time lag in its response to rainfall, of about 1 h, for all

age-classes. Yet the magnitude of the response of the stem sap flow of *H. ammodendron* to rainfall was inconsistent among *H*10, *H*15, and *H*20, for which the overall response by age could be ranked as follows: *H*15>*H*10>*H*20.

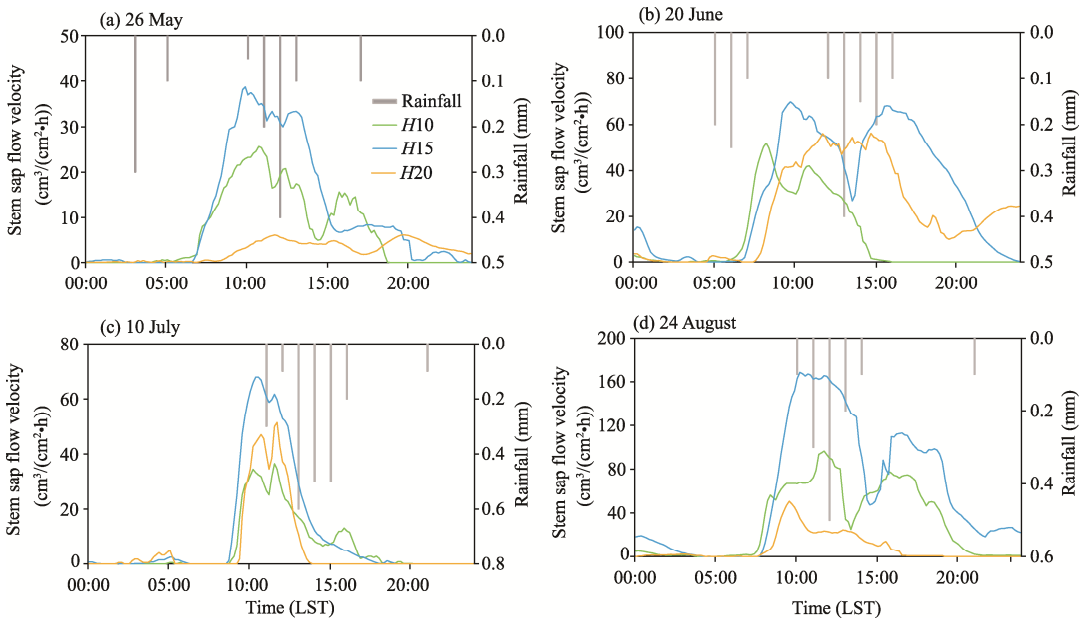

Fig. 4 Hourly dynamics in the stem sap flow velocity of *H. ammodendron* at different ages (*H*10, *H*15, and *H*20) on rainy days of 26 May (a), 20 June (b), 10 July (c), and 24 August (d).

3.3 Daily dynamics in the stem sap flow velocity of *H. ammodendron* at different ages

Daily dynamics in the stem sap flow velocity were compared among the three age-classes of *H. ammodendron* during the growing season (from 1 May to 31 October) (Fig. 5). The stem sap flow velocity of *H. ammodendron* at *H*10 showed an overall trend of initially rising and then declining, which peaked at 112.28 $cm^3/(cm^2 \cdot d)$ on 28 August, and decreased sharply afterwards in October. The stem sap flow velocity of *H. ammodendron* at *H*15 showed a multi-peak pattern; these peaks appeared on 17 June, 19 July, and 18 September, with corresponding values of 227.11, 188.70, and 288.79 $cm^3/(cm^2 \cdot d)$, respectively. The stem sap flow velocity of *H. ammodendron* at *H*20 fluctuated greatly in May and its overall trend was one of increasing then decreasing, which peaked at 119.01 $cm^3/(cm^2 \cdot d)$ on 11 August and then decreased sharply in September.

3.4 Variation in water consumption of *H. ammodendron* at different ages

Figure 6 shows the average daily and total water consumption of *H. ammodendron* at three age-classes (*H*10, *H*15, and *H*20) during the growing season of 2020. The average daily water consumption was highest in May, irrespective of the age-class, with maximal values of 5.6, 5.2 and 3.6 kg/d for *H*10, *H*15, and *H*20, respectively. Across the entire growing season, the average daily water consumption of *H. ammodendron* for *H*15 differed significantly from that for *H*10 or *H*20, with the values of 1.9, 2.8, and 1.9kg/d for *H*10, *H*15, and *H*20, respectively. The total water consumption of *H. ammodendron* in the growing season was 357.3, 509.1, and 344.3 kg for *H*10, *H*15, and *H*20, respectively.

3.5 Correlations between the stem sap flow velocity of *H. ammodendron* at different ages and physical factors

3.5.1 Relationships between the stem flow sap velocity of different-aged *H. ammodendron* and meteorological factors

During the growing season, daily variation data of the stem flow sap velocity of *H. ammodendron* at different ages (*H*10, *H*15, and *H*20) for four consecutive days of each month (19–22 May,

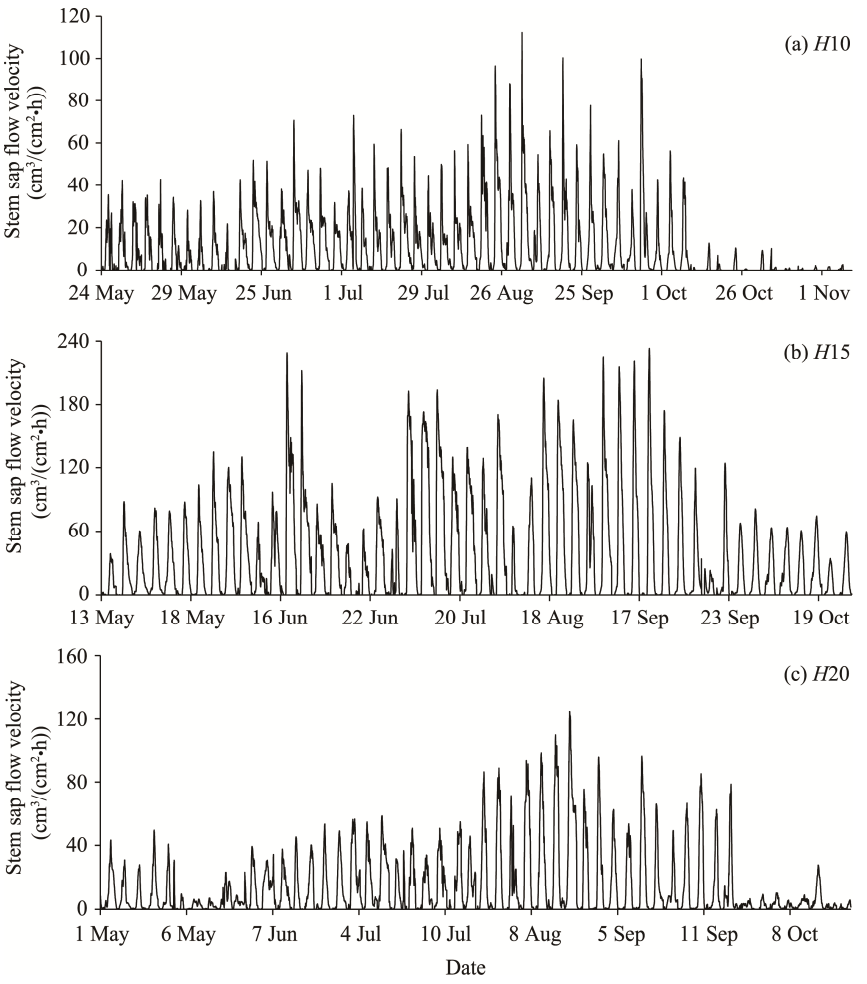

Fig. 5 Daily dynamics in the stem sap flow velocity of *H. ammodendron* at different ages (*H*10, *H*15, and *H*20) during the growing season from 1 May to 31 October. (a), *H*10; (b) *H*15; (c), *H*20.

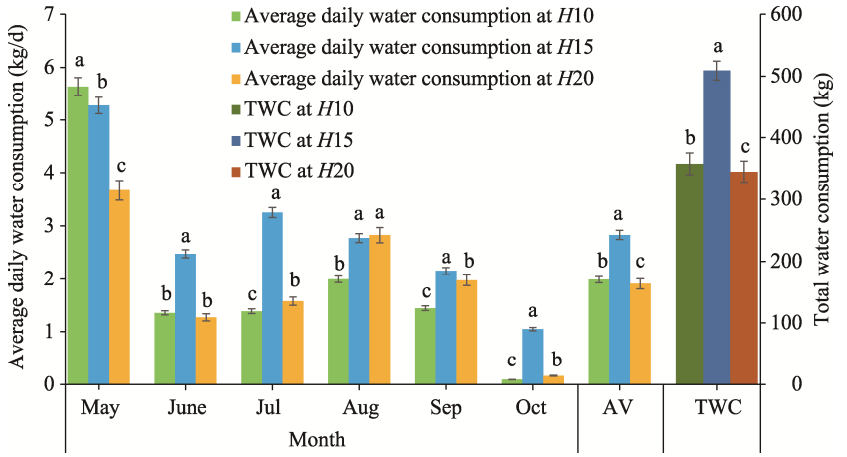

Fig. 6 Variations in the average daily water consumption of *H. ammodendron* at different ages (*H*10, *H*15, and *H*20) in each month of the growing season (from May to October) as well as the total water consumption. AV is the average daily water consumption averaged throughout the growing season, and TWC is the total water consumption throughout the growing season. In the analysis of variance, different lowercase letters indicate significant difference at $P<0.05$ level among the *H. ammodendron* at different ages for the same period. Bars mean standard errors.

16–19 June, 14–17 July, 19–22 August, 14–17 September, and 19–22 October) were selected, along with corresponding meteorological data (temperature, RH, *Rn*, wind speed, and VPD), to fit the SEM. As seen in Table 2, both the Kronbach and KMO test coefficients of the variables for *H*10, *H*15, and *H*20 surpassed the minimum acceptable values; hence, the correlations between the variables were deemed reliable. The second-order validation factor analysis of the SEM theoretical model was performed (using MPLUS 8.0 software), and these results demonstrated that the SEM combined model fitted well: χ^2/df=1.202, RMSEA=0.049, SRMR=0.073, CFI=0.984, and TLI=0.927. According to previous research (Sun et al., 2007), the smaller the value of χ^2, the better the effect; the applicable criteria for CFI and TLI are greater than 0.900, and the minimum acceptable criteria for RMSEA and SRMR are lower than 0.090. Therefore, all metrics satisfied the critical value requirements for establishing the SEM model's goodness-of-fit.

Table 2 Reliability and validity test statistics of sample data for the structural equation model (SEM) for *H. ammodendron* at different ages (*H*10, *H*15, and *H*20)

Forest stand	Variable	*N*	Cronbach's Alpha	KMO
*H*10	Meteorological factors	5	0.716	0.784
*H*15	Meteorological factors	5	0.803	0.722
*H*20	Meteorological factors	5	0.701	0.677

Note: *H*10, *H*15, and *H*20 are *H. ammodendron* forest stands with different afforestation ages of 10, 15, and 20 years old, respectively. *N*, number of measurable variables; KMO, Kaiser-Meyer-Olkin.

In Figure 7, meteorological factors were clearly correlated with the stem sap flow velocity of *H. ammodendron* at different ages. According to Table 3, in considering the respective effects of meteorological factors on the stem sap flow velocity of *H. ammodendron*, temperature had the largest weight; hence, temperature was the key factor affecting the stem sap flow of *H. ammodendron*. The effects of the five meteorological factors upon the stem sap flow velocity of different-aged *H. ammodendron* plants can be ranked as follows: temperature>*Rn*>VPD>wind speed>RH for *H*10 and *H*15, and temperature>VPD>*Rn*>wind speed>RH for *H*20 (Table 3).

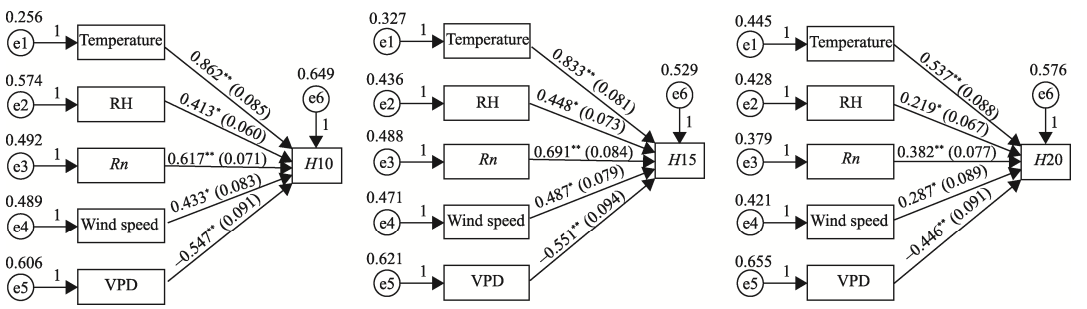

Fig. 7 Path diagram of the structural equation model (SEM) showing the response of the stem flow velocity of *H. ammodendron* to meteorological factors during the growing season. ** indicates statistically significant correlation at P<0.01 level; * indicates statistically significant correlation at P<0.05 level; e1 to e6 represent residual variables; the number 1 represents the factor load; the value in parentheses represents the root mean square of the residuals ; the variable pointed by the arrow is an endogenous variable.

Table 3 Calculation results of the meteorological factors' weights for *H. ammodendron* at different ages (*H*10, *H*15, and *H*20)

Criterion layer	Index layer	Weight		
		*H*10	*H*15	*H*20
Meteorological factors	Temperature	0.300	0.277	0.284
	RH	0.143	0.149	0.116
	Rn	0.214	0.229	0.202
	Wind speed	0.151	0.162	0.152
	VPD	0.192	0.183	0.246

Note: RH, relative humidity; *Rn*, net radiation; VPD, vapor pressure deficit.

Moreover, the stem sap flow velocity of *H. ammodendron* at the three age-classes showed correlations with various meteorological factors under different weather conditions (Table 4), and these correlations were significantly greater on sunny days than on rainy days. Under sunny conditions, VPD was the main factor influencing the stem sap flow velocity. The correlations between stem sap flow velocity and meteorological factors changed across months and shifted among different ages. Rainfall showed a very significant correlation with stem sap flow velocity (P<0.01), for which the ranking of correlation coefficients was *H*15>*H*20>*H*10.

Table 4 Correlation analysis of hourly-scale stem sap flow velocity of *H. ammodendron* at different ages (*H*10, *H*15, and *H*20) and meteorological factors

	Forest stand	Weather	Temperature	RH	*Rn*	VPD	Wind speed
Stem sap flow velocity	*H*10	Sunny days	0.728**	–0.755**	0.812**	–0.745**	0.517**
		Rainy days	0.329	–0.518**	0.523**	–0.547**	0.451**
	*H*15	Sunny days	0.625**	–0.691**	0.665**	–0.769**	0.646**
		Rainy days	0.437*	–0.457**	0.417**	–0.542**	0.648**
	*H*20	Sunny days	0.553**	–0.517*	0.676**	–0.684**	0.531**
		Rainy days	0.409*	–0.423**	0.551**	–0.453**	0.515**

Note: ** indicates statistically significant correlation at P<0.01 level; * indicates statistically significant correlation at P<0.05 level.

3.5.2 Relationships between the stem sap flow velocity of different-aged *H. ammodendron* and soil moisture

On sunny days, the stem sap flow velocity of *H. ammodendron* at each age-class had very significant correlations with soil moisture at soil depths of 50 and 100 cm (Table 5). Specifically, stem sap flow velocity and soil moisture were negatively correlated in the upper soil depth, and positively correlated in the deeper soil depth. Moreover, the correlation coefficients on sunny days were ranked as *H*10>*H*15>*H*20. On rainy days, in contrast, the correlations between stem sap flow velocity and soil moisture were weaker and not significant.

Table 5 Correlation analysis between the stem sap flow velocity of *H. ammodendron* at different ages (*H*10, *H*15, and *H*20) and soil moisture at different depths

		Stem sap flow velocity					
		Sunny days			Rainy days		
		*H*10	*H*15	*H*20	*H*10	*H*15	*H*20
Soil moisture	5 cm	0.012	–0.158	0.162	0.243	0.216	0.284
	20 cm	–0.049	–0.237	0.109	0.182	0.155	0.171
	50 cm	–0.760**	–0.523**	–0.429**	0.291	0.227	0.174
	100 cm	0.736**	0.674**	0.589**	0.194	0.215	0.248

Note: ** indicates statistically significant correlation at P<0.01 level.

4 Discussion

4.1 Variation in the stem sap flow velocity of *H. ammodendron* at different ages

In May, compared with *H*10 and *H*20, the stem sap flow velocity of *H. ammodendron* plants at *H*15 was larger and their stem sap flow started earlier but ended later in a day. The reason for this is that the crown canopy diameter of *H. ammodendron* plants at *H*15 was relatively large (Table 1). Moreover, the temperature at the forest stand was suitable in May (Fig. 2), and winds were more frequent then (Guo et al., 2016). These winds reduced the humidity around the leaves of *H. ammodendron*, affecting the stem sap flow velocity by increasing the VPD, and May's suitable natural conditions resulted in greater stem sap flow velocity *H. ammodendron* plants at *H*15 in that month. Recently, Xia et al. (2019) reported that the stem sap flow velocity of 'Hanfu' apple

trees showed a single-peak "Z" shape change and its value was higher in the daytime and lower at night. In this study, we found that the hourly variation curves of the stem sap flow velocity of *H. ammodendron* at the three age-classes under sunny conditions were mainly unimodal, with weak peak at night and significant hourly differences. A similar conclusion was also drawn for *Elaeagnus angustifolia* (Liu et al., 2021). In May, the stem sap flow of *H. ammodendron* plants at *H*20 started late and ended early, and their flow velocity peaked later, with the values significantly smaller than that of *H. ammodendron* plants at *H*10 and *H*15 at the germination stage of their newly assimilated branches. A plausible explanation for this is the low rainfall and soil moisture in May and June. Furthermore, *H. ammodendron* plants at *H*20 showed signs of branch dieback and rodent damage (Luo et al., 2017), pests, and diseases (Ma et al., 2012), as well as the natural dieback of their own branches in this water-scarce environment. Collectively, this led to smaller crown diameter size (Table 1), decreased surface accumulation, poor water-holding capacity, and reliance on groundwater for most of the water sources these plants used.

In October, the temperature dropped sharply, the self-metabolism of *H. ammodendron* plants slowed, and their absorption and transpiration of soil moisture decreased. The stem sap flow velocity of *H. ammodendron* plants was starkly different among *H*10, *H*15, and *H*20. On sunny days, their hourly variation curves mainly displayed a single peak, with weak stem sap flow at night, and the difference between daytime and night was significant. On rainy days, the stem sap flow velocity of different-aged *H. ammodendron* plants was significantly lower than that on sunny days, and could be ranked as *H*15>*H*10>*H*20. The reason for this phenomenon is that the canopy of *H. ammodendron* plants can directly absorb water during rainy days and then contribute to the stem sap flow. The larger the crown canopy diameter, the more water it can absorb. This result is consistent with earlier findings of Xia et al. (2014) and Yue et al. (2020) on the water consumption dynamics of *H. ammodendron* in the Gurbantunggut Desert, China.

4.2 Variation in the water consumption of *H. ammodendron* at different ages

In May, the average daily water consumption of *H. ammodendron* plants at different ages (*H*10, *H*15, and *H*20) reached the maximum, likely because of a confluence of factors. In the study area, the plants' branches started to sprout in April (Zhang et al., 2021), the temperature varied between 5.0°C and 25.0°C, and the weather was windiest in May. This windy weather increased the transpiration rate of *H. ammodendron*, which together with the stronger photosynthetic effective radiation and frequent rainfall created suitable environmental conditions, allowing for the rapid development and growth of the rhizomes and assimilated branches of *H. ammodendron* (Fig. 3). Similarly, Jia et al. (2020) argued that due to the timing of the rainy season and drought stress, the maximum water consumption of some shrubs actually occurs in May. However, work by Cao et al. (2013) and Zhang et al. (2016) concluded that the maximum water consumption by *H. ammodendron* occurs in July. That discrepancy with our study can be explained by the different rainfall and temperature regimes during the observation period among studies, given that temperature and rainfall are key factors known to determine the water consumption of *H. ammodendron* plants. We found that temperatures were highest in June and July during the observation period when rainfall was scarce. Accordingly, this higher temperature would have promoted the stomata closure of *H. ammodendron*, thereby reducing photosynthesis and slowing the material conversion and energy metabolism of plants, which entails consuming less water. In June and July, compared with *H*10 or *H*20, *H. ammodendron* plants at *H*15 consumed much more water, because they had larger canopy diameter and transpired strongly at high temperatures. The most rainfall occurred in September, when the average daily water consumption of *H. ammodendron* at the three age-classes was rather low. Because the temperature decreased and diurnal temperature difference was so large in September, photosynthetic effective radiation was diminished and the abscisic acid content of *H. ammodendron* was at its greatest level (Ma et al., 2012). This would have cued *H. ammodendron* plants to enter dormancy (Zhao et al., 2017; Gao et al., 2020), thus leading to low water consumption.

By comparing the water consumption of *H. ammodendron* in different regions (Table 6), we

found that the water consumption of *H. ammodendron* plants at *H*10 and *H*20 in our study area was similar to that of *H. ammodendron* plants native to the Gurbantunggut Desert, China, while the water consumption of *H. ammodendron* plants at *H*15 in our study area was on par with the water consumption of *H. ammodendron* plants native to the Badain Jaran Desert, China.

Table 6 Comparison of the water consumption of *H. ammodendron* plants studied in the different regions

H. ammodendron type	Monitoring time	Place	Method	Diameter (cm)	Daily water consumption (kg/d)	Total water consumption (kg)	Reference
Native	April to September	Gurbantunggut Desert, China	HPV	7.80–9.00	2.50–4.60	400–500	Sun et al. (2010)
Native	June to November	Badain Jaran Desert, China	TMD	9.90–13.66	2.50–4.61	400–501	Zhang et al. (2017)
Native	May to September	Gurbantunggut Desert, China	TMD	4.55–9.55	2.50–4.62	400–502	Li et al. (2017)
Artificial	May to September	Ulan Buhe Desert, China	TMD	7.00–12.50	2.50–4.63	400–503	Huang et al. (2020)
Artificial	June to September	Shihezi University Agricultural testing ground, China	TMD	15.70–21.50	2.50–4.64	400–504	Yang et al. (2018)

Note: HPV, an insertion sensor that measures stem sap flow velocity by using the thermal pulse method; TMD, thermal diffusion method.

Previous research has shown that the *H. ammodendron* plantations may undergo a pronounced self-thinning process after more than 10 years (Song et al., 2021; Zhao et al., 2023). For *H. ammodendron* plantation at *H*10 in this study, the number of surviving plants decreased, the shrub belt structure disappeared, and the soil water consumption of the entire plant community gradually declined (Song et al., 2021; Liu et al., 2022). Consequently, for *H. ammodendron* plantation at *H*15, there were only a few plants remaining but soil water consumption was better balanced. Further experimental findings showed that, even though *H. ammodendron* plants at *H*20 can use groundwater, their mortality rate in the plantation was still high. Hence, the death rate of *H. ammodendron* plants increased with stand age.

4.3 Responses of the stem sap flow velocity of *H. ammodendron* at different ages to physical factors

Temperature was the key factor governing the stem sap flow velocity of *H. ammodendron*. In the effective temperature range, as the temperature rose, the growth rate of *H. ammodendron* plants accelerated. When the temperature reached the light saturation point, *H. ammodendron* reached its maximum water consumption (Sun et al., 2010; Mahdavi et al., 2022), so temperature had a high weight among the meteorological factors (Table 3). *Rn* influenced the photosynthetic rate of *H. ammodendron*, and as a heat source, this net surface radiation warmed or cooled the surface and advective atmosphere, with heat consumed by evaporation and transpiration (Dong, 2013). In this way, the influence of *Rn* upon the stem sap flow velocity of *H. ammodendron* plants at *H*10 and *H*15 took on a high weight. The leaf stomata were pores consisting of a pair of guard cells, which functioned as key links in regulating the exchange of materials and energy such as water and CO_2 between plants and their external environment; thus, stomatal changes profoundly affected transpiration and photosynthesis rates (Xia et al., 2014). VPD reflected the degree of atmospheric aridity and evaporative stress of plants (Yang et al., 2018). When the air humidity decreased, the stomata closed due to the increase of VPD, which altered the stem sap flow velocity of *H. ammodendron*. In this way, VPD indirectly improved photosynthetic performance, so it took on a high weight for *H. ammodendron* plants at *H*20. Although both wind speed and RH exerted some influence on the stem sap flow velocity of *H. ammodendron*, their corresponding weights were much lower.

Under sunny conditions, the stem sap flow velocity of *H. ammodendron* and soil moisture at the depths of 50 and 100 cm showed strong significant correlation. The younger the stand age of *H. ammodendron* plants, the more significant was the correlation. The reason for this is that the

soil layer at the depth of 0–100 cm in the study area consisted of sandy soil with a poor water-holding capacity (Guo et al., 2016). Underground of the study area at the 100 cm depth belowground did have a certain water-holding capacity, and the depth at which roots of *H. ammodendron* consumed water increased with stand age (Zhang et al., 2016). Therefore, the older the stand age of this species, the better was the correlation between the stem sap flow velocity and soil moisture in the deep layer. At 50 cm belowground, the stem sap flow velocity of *H. ammodendron* plants at the three age-classes (*H*10, *H*15, and *H*20) showed a very significant negative correlation with soil moisture. This result could be due to the fact that sandy soils in the top 50 cm depth layer were involved in surface evaporation in the face of high temperatures, thus reducing water availability around the root system of *H. ammodendron* and inhibiting its water consumption (Zhou et al., 2017). At the 100 cm belowground, the stem sap flow velocity of *H. ammodendron* and soil moisture were significantly positively correlated, indicating that the soil in the layer below 100 cm in the study area had an ability to retain water, and that most of the water-absorbing roots of *H. ammodendron* were distributed below 100 cm ground (Xu et al., 2021).

5 Conclusions

This study's results showed that the hourly curves of the stem sap flow velocity of *H. ammodendron* features a single peak on sunny days and multiple peak on rainy days. The magnitude of the stem sap flow velocity is significantly lower on rainy days than on sunny days. Temperature is the chief factor affecting the shifts in the stem sap flow velocity of *H. ammodendron*, whose correlation is more significant in younger stands. The older the stand age of these plants, the deeper is their use of soil moisture. The water consumption of *H. ammodendron* plants in the Minqin oasis-desert transition zone reaches its maximum at an age of 15 years old (*H*15), compared to the *H*10 and *H*20. Although *H. ammodendron* plants in *H*20 could use groundwater, its water consumption is low and its mortality rate likely very high. This may be because the water consumption of *H. ammodendron* plants causes the groundwater level to drop, such that the groundwater absorbed by *H. ammodendron* plants is insufficient to maintain their physiological activity. Therefore, the initial density of *H. ammodendron* forest stands must be reasonably planned to mitigate their future consumption of valuable soil moisture in arid regions, so as to maintain the stability of *H. ammodendron* plantations there and facilitate greater ecological benefits.

Conflict of interest

The authors declare that they have no known competing financial interests or personal relationships that could have appeared to influence the work reported in this paper.

Acknowledgements

This study was supported by the National Natural Science Foundation of China Subsidization Project (32260425, 31860238) and the Natural Science Foundation of Gansu Province, China (32060246, 21JR7RA733).

Author contributions

XU Xianying and ZHANG Jinchun designed the experiment. ZHANG Jinchun provided funding for this study. QIANG Yuquan, LIU Hujun and DUAN Xiaofeng completed the experiment and QIANG Yuquan wrote the manuscript.

References

Cao L, Nie Z L, Liu M, et al. 2021. The ecological relationship of groundwater-soil-vegetation in the oasis-desert transition zone of the Shiyang River Basin. Water, 13(12): 1642, doi: 10.3390/w13121642.

Cao X M, Chen X, Wang J L. 2013. Transpiration and water consumption characteristics of *Haloxylon ammodendron* under non irrigation conditions in the southern edge of Gurbantunggut. Arid Land Geography, 36(2): 292–302. (in Chinese)

Chang Z F, Zhao M, Liu H J. 2007. Study on dynamic characteristics of desert ecological degradation in Minqin. Chinese Agricultural Science Bulletin, 23(11): 333–338. (in Chinese)

Ding A Q. 2018. Study on vegetation community and soil characteristics of degraded *Tamarix* shrub sand pile in Minqin Oasis-Desert transition zone. MSc Thesis. Beijing: Chinese Academy of Forestry. (in Chinese)

Dong M. 2013. Physiological study on drought and salt tolerance of main tree species in Qaidam area. MSc Thesis. Beijing: Beijing Forestry University. (in Chinese)

Gao H J, Lü X P, Ren W, et al. 2020. *HaASR1* gene cloned from a desert shrub, *Haloxylon ammodendron*, confers drought tolerance in transgenic *Arabidopsis thaliana*. Environmental and Experimental Botany, 180: 104251, doi: 10.1016/j.envexpbot.2020.104251.

Granier A. 1987. Sap flow measurements in Douglas-fir tree trunks by means of a new thermal method. Annales des Sciences Forestières, 44(1): 1–14. (in French)

Guo S J, Yang Z H, Wang D Z, et al. 2016. Distribution characteristics of aeolian dust near Qingtu Lake in the lower reaches of Shiyang River. Arid Land Geography, 39(6): 1255–1262. (in Chinese)

He A L, Niu S Q, Zhao Q, et al. 2018. Induced salt tolerance of perennial ryegrass by a novel bacterium strain from the rhizosphere of a desert shrub *Haloxylon ammodendron*. International Journal of Molecular Sciences, 19(2): 469, doi: 10.3390/ijms19020469.

Hu D, Lü G H, Qie Y D, et al. 2021. Response of morphological characters and photosynthetic characteristics of *Haloxylon ammodendron* to water and salt stress. Sustainability, 13(1): 388, doi: 10.3390/su13010388.

Huang Y R, Xin Z M, Li Y H, et al. 2020. Seasonal variation of stem sap flow of artificial *Haloxylon ammodendron* in Ulanbuhe Desert and its relationship with meteorological factors. Journal of Nanjing Forestry University, 44(06): 131–139. (in Chinese)

Jia T Y. 2020. Study on transpiration water consumption law and scale effect of shrub semi shrub tree in Horqin sandy land. MSc Thesis. Hohhot: Inner Mongolia Agricultural University. (in Chinese)

Jiang X J., Liu W J, Chen C F, et al. 2018. Effects of three morphometric features of roots on soil water flow behavior in three sites in China. Geoderma, 320: 161–171.

Li H, Hu S J, Zhu H, et al. 2017. Study on sap flow characteristics of *Haloxylon ammodendron* stem based on thermal diffusion technology. Acta Ecologica Sinica, 37(21): 7187–7196. (in Chinese)

Li Y Y, Ma X L, Zhao J L, et al. 2015. Developmental genetic mechanisms of C_4 syndrome based on transcriptome analysis of C_3 cotyledons and C_4 assimilating shoots in *Haloxylon ammodendron*. PLoS ONE, 10(2): e0117175, doi: 10.1371/journal.pone.0117175.

Liu P F, Guo H, Xin Z M. 2021. The relationship between the stem sap flow of *Elaeagnus angustifolia* Linn. and environmental factors in Ulan Buh Desert. Journal of Arid Land Resources and Environment, 35(09): 177–184. (in Chinese)

Liu Y Z, Zeng Y, Yang Y H, et al. 2022. Competition, spatial pattern, and regeneration of *Haloxylon ammodendron* and *Haloxylon persicum* communities in the Gurbantunggut Desert, Northwest China. Journal of Arid Land, 14(10): 1138–1158.

Lu J Q, Zhang X F, Liang S M, et al. 2023. Spatiotemporal dynamics of vegetation index in an oasis-desert transition zone and relationship with environmental factors. Sustainability, 15(4): 3503, doi: 10.3390/su15043503.

Luo Q H, Chen Q M, Ning H S, et al. 2017. Chronosequence-based population structure and natural regeneration of *Haloxylon ammodendron* plantation in the southern edge of the Gurbantunggut Desert, Northwestern China. Russian Journal of Ecology, 48(4): 364–371.

Lü X P, Gao H J, Zhang L, et al. 2019. Dynamic responses of *Haloxylon ammodendron* to various degrees of simulated drought stress. Plant Physiol Bioch, 139: 121–131.

Ma C S, Gu Z D, Li J J, et al. 2012. Occurrence types and control countermeasures of *Haloxylon ammodendron* plantation in arid desert area in the lower reaches of Shiyang River. Gansu Forestry Science and Technology, 37(3): 36–39. (in Chinese)

Mahdavi S M, Latifi M, Asadi M, et al. 2022. A new species of *Augeriflechtmannia* (Prostigmata: Tetranychidae) from *Haloxylon ammodendron* (Amaranthaceae) in Iran and a key to the world species. Acarologia, 62(4): 898–907.

Ning T T, Li Z, Feng Q, et al. 2020. Effects of forest cover change on catchment evapotranspiration variation in China. Hydrological Processes, 34(10): 2219–2228.

Pan X L. 2000. Thoughts on the study of ecological environment evolution and regulation in arid areas in western China. World Science and Technology Research and Development, 22(3): 57–60. (in Chinese)

Poyatos R, Granda V, Flo V, et al. 2021. Global transpiration data from sap flow measurements: the SAPFLUXNET database. Earth System Science Data, 13(6): 2607–2649.

Song C W, Li C J, Halik Ü, et al. 2021. Spatial distribution and structural characteristics for *Haloxylon ammodendron* plantation on the southwestern edge of the Gurbantünggüt Desert. Forests, 12(5): 633, doi: 10.3390/f12050633.

Sun P F, Zhou H F, Li Y, et al. 2010. Sap flow and water consumption of native *Haloxylon ammodendron* in Gurbantunggut Desert. Acta Ecologica Sinica, 30(24): 6901–6909. (in Chinese)

Sun W, Chou C P, Stacy A W, et al. 2007. SAS and SPSS macros to calculate standardized Cronbach's alpha using the upper bound of the phi coefficient for dichotomous items. Behavior Research Methods, 39(1): 71–81.

Thomas F M, Foetzki A, Arndt S K, et al. 2006. Water use by perennial plants in the transition zone between river oasis and desert in NW China. Basic and Applied Ecology, 7(3): 253–267.

Wang W H, Chen Y N, Wang W R, et al. 2023. Water quality and interaction between groundwater and surface water impacted by agricultural activities in an oasis-desert region. Journal of Hydrology, 617: 128937, doi: 10.1016/j.jhydrol.2022.128937.

Wang Y, Li C, Li A D, et al. 2015. Relationship between degradation of *Nitraria repens* and soil moisture. Acta Ecologica Sinica, 35(5): 1407–1421. (in Chinese)

Xia G M, Sun Y Y, Wang W Z, et al. 2019. "Hanfu" apple tree stem flow characteristics and its response to environmental factors. Scientia Agricultura Sinica, 52(04): 701–714. (in Chinese)

Xia Y H, Liang F C, Shi Q D, et al. 2014. Study on transpiration water consumption of *Haloxylon ammodendron* native desert vegetation in artificial carbon sink forest in western Junggar. Journal of Anhui Agricultural Sciences, 42(33): 11755–11759. (in Chinese)

Xu G Q, Mi X J, Ma J, et al. 2021. Impact of groundwater depth on hydraulic performance and growth of *Haloxylon ammodendron* in a desert region of central Asia. Ecohydrology, 15(5): e2394, doi: 10.1002/eco.2394.

Yang J X, Zhao J, Zhu G F, et al. 2020. Soil salinization in the oasis areas of downstream inland rivers—Case study: Minqin oasis. Quaternary International, 537: 69–78.

Yang M J, Yang G, He X L, et al. 2018. Stem sap flow characteristics of *Haloxylon ammodendron* in arid area and its response to soil moisture. Yangtze River, 49(6): 33–38. (in Chinese)

Yue Y M, Li C H, Xu Z, et al. 2020. Variation characteristics of canopy nutrients of *Haloxylon ammodendron* and *Haloxylon persicum* during rainfall in Gurbantunggut. Arid Zone Research, 37(5): 1293–1300. (in Chinese)

Zhang K, Su Y Z, Liu T N, et al. 2016. Leaf C: N: P stoichiometrical and morphological traits of *Haloxylon ammodendron* over plantation age sequences in an oasis-desert ecotone in North China. Ecological Research, 31(3): 449–457.

Zhang Q D, Liu W, Bai B, et al. 2019. Study on ecological characteristics of *Haloxylon ammodendron* plantation at different forest ages in yiliangtan Minqin. Protection Forest Science and Technology, (11): 14–16. (in Chinese)

Zhang W L, Zhao P, Zhu S J, et al. 2021. Seasonal variation of water use strategy of artificial *Haloxylon ammodendron* in the lower reaches of Shiyang River. Pratacultural Science, 38(05): 880–889.

Zhang X Y, Chu J M, Meng P, et al. 2016. Effects of environmental factors on evapotranspiration characteristics of *Haloxylon ammodendron* plantation in the Minqin oasis-desert ecotone, Northwest China. Chinese Journal of Applied Ecology, 27(8): 2390–2400. (in Chinese)

Zhang X Y, Chu J M, Meng P, et al. 2017. Stem sap flow characteristics of *Haloxylon ammodendron* (C.A. Mey) Bunge in Minqin Oasis-Desert transition zone and its response to environmental factors. Acta Ecologica Sinica, 37(5): 1525–1536. (in Chinese)

Zhao P, Xu X Y, Qu J J, et al. 2017. Relationship between artificial *Haloxylon ammodendron* community and soil and water factors in Minqin Oasis-Desert transition zone. Acta Ecologica Sinica, 37(5): 1496–1505. (in Chinese)

Zhao W Y, Ji X B, Jin B W, et al. 2023. Experimental partitioning of rainfall into throughfall, stemflow and interception loss by *Haloxylon ammodendron*, a dominant sand-stabilizing shrub in northwestern China. Science of The Total Environment, 858: 159928, doi: 10.1016/j.scitotenv.2022.159928.

Zheng C L, Wang Q. 2015. Seasonal and annual variation in transpiration of a dominant desert species, *Haloxylon ammodendron*, in Central Asia up-scaled from sap flow measurement. Ecohydrology, 8(5): 948–960.

Zhou H, Zhao W Z, Zhang G F. 2017. Varying water utilization of *Haloxylon ammodendron* plantations in a desert-oasis ecotone. Hydrol Processes, 31(4):825–835.

Zhu Y J, Jia Z Q. 2011. Soil water utilization characteristics of *Haloxylon ammodendron* plantation with different age during summer. Acta Ecologica Sinica, 31(6): 341–346.